Multiconical emission at light counterpropagation in a resonant medium

A. A. Afanas'ev and B. A. Samson
Institute of Physics, Belarus Academy of Sciences, 70 F. Skaryna Avenue, Minsk 220072, Belarus
(Received 27 September 1994; revised manuscript received 16 December 1994)

We describe one of the possible ways of development of a spatial instability of counterpropagating strong light beams in resonant media. The interplay between self-focusing and saturation effects results in a formation of counterpropagating stable filaments. The nondegenerate four-photon scattering in these waveguiding structures leads to a far-field multiconical emission with the cones' frequencies shifted to both red and blue sides of the resonant transition.

PACS number(s): 42.50.SF

I. INTRODUCTION

The counterpropagation of strong light beams in nonlinear media is capable of demonstrating a large variety of instability effects. The temporal instability can lead to an excitation of regular pulsations and chaos [1–4]; the spatial one can result in the formation of patterns of different symmetries and turbulence in the transverse beam section [2,5–9]. Resonant media, due to their spectral-selective and saturation properties, enrich nonlinear light behavior comparatively with Kerr-like nonlinearity. For example, at copropagation of a light beam with frequency on the blue side of a resonant transition, an emission with frequency on the red side is excited, forming a far-field ring structure (see, for example, [10]). This effect has been called conical emission and is intrinsic for to resonant media spatial instability. The conical emission, as it has been shown in [11,12], appears mainly due to a frequency-shifted four-photon scattering on Stark sublevels of the resonant system. The emission is excited inside stable light filaments, resulting in the development of a self-focusing frequency-nondegenerate spatial instability.

Counterpropagation in resonant media yields, generally, the formation of filaments as well. It should be noted that the problem concerning the interaction of counterpropagating guided waves leading to their cross-trapping has been considered in [13], and several aspects of the interaction of self-trapped counterpropagating channels, resulting in so-called cross-induced self-focusing bistability, were regarded in [14]. We will show below that the filaments coming from opposite directions attract each other. As the result of evolution, the system is capable of forming a composite filament, consisting of two counterpropagating ones. Moreover, it is known [15] that among the whole family of such spatial structures the filaments with insufficiently distinguished total energies of the components are most stable.

That allows us to consider the formation of the filaments as one of the intermediate asymptotics in the development of instability of counterpropagating beams. The purpose of this work is to elucidate properties of the following stage, namely, the four-photon frequency-shifted decay of the counterpropagating filaments. This instability shows itself in far field as colored rings around the central pump spots. That corresponds to emission of the scattered radiation in cones at several angles with respect to the filament propagation direction. The cone frequencies, unlike in the copropagation case, lie on both sides of the resonant transition, blue and red.

II. INTERACTION OF COUNTERPROPAGATING FILAMENTS

It is well known that the spatial frequency-degenerate instability of a strong light beam in resonant media can result in the formation of stable spatial structures, filaments, or spatial solitons as they were called quite recently. That occurs under several conditions, namely, positive frequency detuning of the light from the resonant transition (blue side) and absence of energy dissipation, which can be supposed when the detuning sufficiently exceeds the resonant linewidth. The stability of the filaments is provided by the saturation mechanism, which also allows the filaments to possess any energy above the self-focusing threshold.

The filaments can be considered as elementary spatial ''quanta'' for the case of counterpropagation as well. There are two kinds of them: composite filaments (CF's), consisting of two counterpropagating components, and simple one-component ones (SF's). In order to elucidate what kind of filament is chosen by the system as more preferable, we should carry out a stability analysis of SF's versus the interaction between them.

We will apply the Lagrange formalism for the following equations describing the counter-propagation of two strong light beams with amplitudes $E_{\pm}(z,\mathbf{r}_{\perp})$ (see Fig. 1) in a resonant medium [15]:

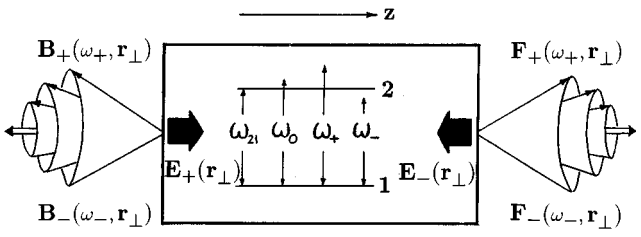

FIG. 1. The scheme of the counterpropagation in a resonant two-level medium. The multiconical emission appears due to the four-photon scattering in the field of composite filaments, formed as the result of a counterpropagating self-focusing of the beams $E_{\pm}(\mathbf{r}_{\perp})$.

$$\pm iE_{\pm z}+\Delta_\perp E_\pm - F(|E_\pm|^2;|E_\mp|^2)E_\pm = 0, \tag{1}$$

where $\Delta_\perp$ is the Laplacian over transverse coordinate $\{\mathbf{r}_\perp\}$. The function

$$F(x;y)=\frac{\rho_0}{\delta}\frac{1}{2x}\left[1-\frac{1+y-x}{\sqrt{1+2x+2y+(x-y)^2}}\right] \tag{2}$$

is the part resonant with the light beams of the nonlinear susceptibility of the medium periodically modulated along z. In the simplest case of nonsaturating fields $x,y\to 0$, the function F takes the usual form for Kerr-like nonlinearity

$$F(x;y)=\frac{\rho_0}{\delta}(1-x-2y). \tag{3}$$

In (2) and (3) ρ_0 is the linear on-line amplitude absorption coefficient and $\delta\gg 1$ is the dimensionless detuning of the light frequency from resonance in linewidth units.

The Lagrangian for (1) after eliminating the linear terms reads

$$L=\int \mathscr{L} d\mathbf{r}_\perp , \tag{4}$$

where

$$\mathscr{L}=i(\dot{E}_+E_+^*-\dot{E}_+^*E_+)-i(\dot{E}_-E_-^*-\dot{E}_-^*E_-)-|\nabla E_+|^2$$
$$-|\nabla E_-|^2+G(|E_+|^2;|E_-|^2)$$

is the Lagrange density, the dot means a derivation on z. We will consider the nonsaturating limit; then the function G takes the form

$$G(|E_+|^2;|E_-|^2)=\tfrac{1}{2}(|E_+|^4+|E_-|^4+4|E_+|^2|E_-|^2).$$

As the next step, we have chosen the trial functions $E_\pm$ of the form

$$E_\pm=\theta_\pm \exp\{-(\gamma_\pm+ik_\pm)[(x-x_\pm)^2+y^2]+i\beta_\pm x\}, \tag{5}$$

where all the values $\theta_\pm$, $\gamma_\pm$, $k_\pm$, $x_\pm$, and $\beta_\pm$ are several unknown functions of z.

Upon substitution of (5) into (4) we obtain the form of the Lagrangian depending on parameters of the trial functions and their derivations. Applying the Euler-Lagrange equations to it we find the set of dynamical equations governing the evolution of the peak intensity $I_\pm=|\theta_\pm|^2$, width $\gamma_\pm$, wave front curvature $k_\pm$, slope $\beta_\pm$, and peak position $x_\pm$:

$$\pm\dot{\gamma}_\pm = 4k_\pm , \tag{6}$$

$$\pm\dot{I}_\pm = 4k_\pm I_\pm , \tag{7}$$

$$\pm\dot{k}_\pm = 2(k_\pm^2-\gamma_\pm^2)+\frac{\gamma_\pm}{4}I_\pm+2I_\mp\frac{\gamma_\pm^2\gamma_\mp}{(\gamma_++\gamma_-)^2}$$
$$\times[1-\gamma_c(x_+-x_-)^2]\exp[-\gamma_c(x_+-x_-)^2], \tag{8}$$

$$\pm\dot{\beta}_\pm = -\frac{I_\mp}{\gamma_\mp}\gamma_c 2(x_\pm-x_\mp)\exp[-\gamma_c(x_+-x_-)^2], \tag{9}$$

$$\pm\dot{x}_\pm = \beta_\pm I_\pm/\gamma_\pm , \tag{10}$$

where

$$\gamma_c = 2\gamma_+\gamma_-/(\gamma_++\gamma_-).$$

It immediately follows from (9) and (10) that the counterpropagating SF's will unidirectionally attract each other, trying to get united into the CF. The unification stage cannot be described in the framework of the nonsaturation limit because of the fixed energies of SF and CF, the so called critical ones. This restriction may be avoided by taking into account just the first saturation terms in the expansion of the functions F and G. Then both SF and CF can contain any energy above the critical one inside them, and the system (6) – (10) describes all stages of unification of SF's into a CF.

So the counterpropagating SF's are unstable with respect to their attraction and formation of a CF. Moreover, as shown in [15], the CF's with not sufficiently distinguished energies of their components are stable. That allows us to consider the CF formation as the next stage of the frequency-degenerate spatial instability development in counter-propagation in resonant media. Obviously, the next step should be made taking into account the frequency-nondegenerate processes leading to decay of a CF.

III. FOUR-PHOTON INSTABILITY OF COMPOSITE FILAMENTS

It has been proven analytically [11], experimentally, and numerically [12] for the case of copropagation in a resonant medium that the frequency-nondegenerate instability of a light beam follows the degenerate one and the main process responsible for that is the four-photon scattering (FPS), enhanced by resonances on Stark sublevels. That allows us to consider the FPS as the most probable mechanism of destruction of the CF.

Let us assume the pump field $\Sigma_\pm E_\pm(\mathbf{r}_\perp,z)\exp(\pm ikz-i\omega_0 t)$ in the form of the CF, which preserves its structure along axis z:

$$E_\pm(\mathbf{r}_\perp,z)=E(\mathbf{r}_\perp)\exp(\pm i\gamma z).$$

We can write the equations for the amplitudes of fields $F_\pm(\mathbf{r}_\perp,z)\exp(ikz-i\omega_\pm t)$ and $B_\pm(\mathbf{r}_\perp,z)\exp(-ikz-i\omega_\pm t)$, coupled with the pump and with each other by the FPS $2\omega_0=\omega_++\omega_-$:

$$iF_{\pm z}+\Delta_\perp F_\pm = \chi_\pm F_\pm+\beta_\pm B_\mp^* + p_\pm F_\mp^* e^{2i\gamma z}+r_\pm B_\pm e^{2i\gamma z},$$

$$-iB_{\pm z}+\Delta_\perp B_\pm = \chi_\pm B_\pm+\beta_\pm F_\mp^* + p_\pm B_\mp^* e^{-2i\gamma z}$$
$$+r_\pm F_\pm e^{-2i\gamma z}. \tag{11}$$

In (11) the coefficients $\chi_{\pm}$ are responsible for a self-action, $\beta_{\pm}$ for a backward FPS, $p_{\pm}$ for a forward FPS, and $r_{\pm}$ for a distributed feedback reflection. We will reproduce the expression for $\chi_{\pm}$ only, because we will use it in further analysis (the other coefficients can be found in [16,1,17–19]):

$$\chi_{\pm}=-i\rho_0\frac{1}{[\nu_{\pm}-(1\mp i\epsilon)](1+\delta^2)}\times\left[\frac{\Omega_{\pm}\mp i\epsilon(1-i\delta)/2}{C_0}-\frac{\Omega_{\pm}\mu_{\pm}}{C_{\pm}\nu_{\pm}}\right], \tag{12}$$

where

$$C_0=\sqrt{1+4I},\quad C_{\pm}=\sqrt{1+4I(1\mp i\epsilon)/\nu_{\pm}},$$

$$\Omega_{\pm}=(1\mp i\epsilon\eta)[1+i(\delta\mp\epsilon)],$$

$$\mu_{\pm}=1\mp i\epsilon\left[\frac{1-i(\delta\pm\epsilon)}{2(1+i\delta)}+1\right],\quad \nu_{\pm}=\Omega_{\pm}\frac{1-i(\delta\pm\epsilon)}{1+\delta^2}.$$

In (12) $\delta=(\omega_0-\omega_{21})T_2$ and $\epsilon=(\omega_+-\omega_0)T_2$ are dimensionless detunings, ω_{21}, T_1 and T_2 are the frequency and longitudinal and transverse relaxation times of the resonant transition, $\eta=T_1/T_2$, $I(\mathbf{r}_\perp)=|E(\mathbf{r}_\perp)|^2$ is the pump intensity in saturation units.

Let us introduce in (11) the following substitutions:

$$\begin{aligned}B_+&=b_+(\mathbf{r}_\perp)\exp i(-\gamma-\Gamma)z,\\ B_-^*&=b_-(\mathbf{r}_\perp)\exp i(\gamma-\Gamma)z,\\ F_+&=f_+(\mathbf{r}_\perp)\exp i(\gamma-\Gamma)z,\\ F_-^*&=f_-(\mathbf{r}_\perp)\exp i(-\gamma-\Gamma)z,\end{aligned} \tag{13}$$

where Γ is a certain propagation constant. Then the system (11) with natural boundary conditions corresponding to an exponential damping of scattered emission at $|\mathbf{r}_\perp|\to\infty$ is reduced to the eighth-order eigenvalue problem for Γ:

$$\begin{aligned}\Delta_\perp f_+&=(\chi_++\gamma-\Gamma)f_++\beta_+b_-+p_+f_-+r_+b_+,\\ \Delta_\perp f_-&=(\chi_-^*+\gamma+\Gamma)f_-+\beta_-^*b_++p_-^*f_++r_-^*b_-,\\ \Delta_\perp b_+&=(\chi_++\gamma+\Gamma)b_++\beta_+f_-+p_+b_-+r_+f_+,\\ \Delta_\perp b_-&=(\chi_-^*+\gamma-\Gamma)b_-+\beta_-^*f_++p_-^*b_++r_-^*f_-.\end{aligned} \tag{14}$$

Problems like (14) were solved numerically in [17,20,19], where different aspects of instability in devices containing counterpropagating beams uniform in the transverse section of the pump beams were considered. The continuity of the eigenvalue spectrum $\{\Gamma\}$, as well as the plane waves $\exp(ik_\perp r_\perp)$ acting as eigenfunctions, allowed one to draw stability diagrams with neutral stability curves given by Im $\Gamma(k_\perp,\mathbf{P})=0$. Here $\mathbf{P}$ is the vector of internal physical parameters, including pump intensity, frequency detunings, etc.; the eigenfunction is usually characterized by the angle θ connected with $k_\perp$ via $k_\perp=k\sin\theta$.

A similar procedure may be carried out in our case. First of all, it should be noted that only damping boundary conditions can ensure an amplification of the fields $F_\pm$ and $B_\pm$ along z. The propagation of untrapped solutions of (14) with finite amplitudes at $|\mathbf{r}_\perp|\to\infty$ is secured by the linear susceptibility $\chi_\pm(|\mathbf{r}_\perp|\to\infty)$ which is generally absorptive. The main feature appearing as a consequence of inhomogeneous pump distribution is creation of a discrete spectrum. Because of the finite transverse size of the pump field the continuous spectrum is responsible for nonlasing solutions, so the instability properties can be established by analyzing the discrete part of the spectrum, corresponding to emission trapped in the CF. Further, the stability diagrams lose one continuous dimension connected with the eigenfunction (in our case $k_\perp$, or, equivalently, θ). Now the equation for the neutral stability $\mathrm{Im}\Gamma_j(\mathbf{P})=0$, where j numerates the eigenvalues, can produce only a discrete set of relations between internal parameters of the problem.

The neutral stability curve will bound the region of the system's internal parameters where the eigenmodes are amplified and, hence, a convective instability occurs. At this stage no boundary conditions $F_\pm(z=0)$ and $B_\pm(z=L)$ (L is the medium length) should be applied. They have to be involved in the consideration of the absolute instability, whose threshold is usually larger than the convective one. Correspondingly, the neutral stability curve $\mathrm{Im}\Gamma_j(\mathbf{P}=0)$ contains a subregion of absolute instability development; the concrete boundaries of the latter strongly depend on the medium length.

We will solve the problem (14) approximately for the one-dimensional case ($\mathbf{r}_\perp\to r_\perp$). Using the Fourier transforms

$$f(r_\perp)=\frac{1}{\sqrt{2\pi}}\int_{-\infty}^{\infty}g(k_\perp)e^{ik_\perp r_\perp}dk_\perp,$$

$$g(k_\perp)=\frac{1}{\sqrt{2\pi}}\int_{-\infty}^{\infty}f(r_\perp)e^{-ik_\perp r_\perp}dr_\perp,$$

$$b(r_\perp)=\frac{1}{\sqrt{2\pi}}\int_{-\infty}^{\infty}a(k_\perp)e^{ik_\perp r_\perp}dk_\perp,$$

$$a(k_\perp)=\frac{1}{\sqrt{2\pi}}\int_{-\infty}^{\infty}b(r_\perp)e^{-ik_\perp r_\perp}dr_\perp,$$

and assuming that the widths of the eigenfunctions $b(r_\perp)$ and $f(r_\perp)$ exceed sufficiently those of the coefficients χ, β, p, and r (which will be confirmed below), we obtain the following system:

$$
\begin{aligned}
-k_\perp^2 g_+ &= (\chi_{+L}+\gamma-\Gamma)g_+ + \chi^k_{+NL} f_+(0) \\
&\quad + \beta^k_+ b_-(0) + p^k_+ f_-(0) + r^k_+ b_+(0), \\
-k_\perp^2 g_- &= (\chi^*_{-L}+\gamma+\Gamma)g_- + \chi^{*k}_{-NL} f_-(0) \\
&\quad + \beta^{k*}_- b_+(0) + p^{k*}_- f_+(0) + r^{k*}_- b_-(0), \\
-k_\perp^2 a_+ &= (\chi_{+L}+\gamma+\Gamma)a_+ + \chi^k_{+NL} b_+(0) \\
&\quad + \beta^k_+ f_-(0) + p^k_+ b_-(0) + r^k_+ f_+(0), \\
-k_\perp^2 a_- &= (\chi^*_{-L}+\gamma-\Gamma)a_- + \chi^{k*}_{-NL} b_-(0) + \beta^{k*}_- f_+(0) \\
&\quad + p^{k*}_- b_+(0) + r^{k*}_- f_-(0).
\end{aligned}
\tag{15}
$$

In (15) we extracted the linear and nonlinear susceptibilities ($\chi=\chi_L+\chi_{NL}$ and $\chi_{NL}\to 0$ at $r_\perp\to\pm\infty$) and introduced the Fourier transforms $\chi^k_{\pm NL}(k_\perp)$, $\beta^k_\pm(k_\perp)$, $p^k_\pm(k_\perp)$, and $r^k_\pm(k_\perp)$ of corresponding spatially inhomogeneous coefficients.

After several manipulations we can obtain a homogeneous system of algebraic equations for $f_\pm(0)$ and $b_\pm(0)$, which has nontrivial solutions under the following condition:

$$
\det(\hat{A}+\sqrt{2\pi}\hat{I})=0, \tag{16}
$$

where

$$
\hat{A}=\begin{pmatrix}
\int_{-\infty}^{\infty}\frac{\chi^k_{+NL}dk_\perp}{k_\perp^2+\gamma-\Gamma+\chi_{+L}} & \int_{-\infty}^{\infty}\frac{p^k_+dk_\perp}{k_\perp^2+\gamma-\Gamma+\chi_{+L}} & \int_{-\infty}^{\infty}\frac{r^k_+dk_\perp}{k_\perp^2+\gamma-\Gamma+\chi_{+L}} & \int_{-\infty}^{\infty}\frac{\beta^k_+dk_\perp}{k_\perp^2+\gamma-\Gamma+\chi_{+L}} \\
\int_{-\infty}^{\infty}\frac{p^{k*}_-dk_\perp}{k_\perp^2+\gamma+\Gamma+\chi^*_{-L}} & \int_{-\infty}^{\infty}\frac{\chi^{k*}_{-NL}dk_\perp}{k_\perp^2+\gamma+\Gamma+\chi^*_{-L}} & \int_{-\infty}^{\infty}\frac{\beta^{k*}_-dk_\perp}{k_\perp^2+\gamma+\Gamma+\chi^*_{-L}} & \int_{-\infty}^{\infty}\frac{r^{k*}_-dk_\perp}{k_\perp^2+\gamma+\Gamma+\chi^*_{-L}} \\
\int_{-\infty}^{\infty}\frac{r^k_+dk_\perp}{k_\perp^2+\gamma+\Gamma+\chi_{+L}} & \int_{-\infty}^{\infty}\frac{\beta^k_+dk_\perp}{k_\perp^2+\gamma+\Gamma+\chi_{+L}} & \int_{-\infty}^{\infty}\frac{\chi^k_{+NL}dk_\perp}{k_\perp^2+\gamma+\Gamma+\chi_{+L}} & \int_{-\infty}^{\infty}\frac{p^k_+dk_\perp}{k_\perp^2+\gamma+\Gamma+\chi_{+L}} \\
\int_{-\infty}^{\infty}\frac{\beta^{k*}_-dk_\perp}{k_\perp^2+\gamma-\Gamma+\chi^*_{-L}} & \int_{-\infty}^{\infty}\frac{r^{k*}_-dk_\perp}{k_\perp^2+\gamma-\Gamma+\chi^*_{-L}} & \int_{-\infty}^{\infty}\frac{p^{k*}_-dk_\perp}{k_\perp^2+\gamma-\Gamma+\chi^*_{-L}} & \int_{-\infty}^{\infty}\frac{\chi^{k*}_{-NL}dk_\perp}{k_\perp^2+\gamma-\Gamma+\chi^*_{-L}}
\end{pmatrix}, \tag{17}
$$

and $\hat{I}$ is the unit 4×4 matrix.

Equation (16) determines the allowed set of eigenvalues $\{\Gamma\}$. In order to solve it, we should calculate the integrals in (17). Let us specify the approximations we used above. The greater width of eigenfunctions than coefficients means

$$
|\mathrm{Im}\sqrt{-\gamma\pm\Gamma-\chi_L}|\ll a^{-1}, \tag{18}
$$

where a is the characteristic scale of transverse variation of the coefficients (it could be much smaller than the filament's transverse size). The stronger condition

$$
|\sqrt{-\gamma\pm\Gamma-\chi_L}|\ll a^{-1} \tag{19}
$$

means a sufficient separation between the poles $k_\perp^0=\pm\sqrt{-\gamma\pm\Gamma-\chi_L}$ and those of the analytically extended coefficients $\chi^k_{\pm NL}(k_\perp)$, $\beta^k_\pm(k_\perp)$, $p^k_\pm(k_\perp)$, $r^k_\pm(k_\perp)$. That allows us to fulfil the integration in (16) on a closed contour, consisting of the real axis $k_\perp\in]-\infty;\infty[$ and the arc of a large radius on the upper complex half plane. We can take into account the contribution of poles $k_\perp^0$ only. After calculations we get an algebraic equation for Γ which can be solved in an approximation of a weak integral nonlinearity,

$$
|\Delta_i^{1/2}|\gg\left|\int_{-\infty}^{\infty}\sigma(r_\perp)dr_\perp\right|, \tag{20}
$$

where σ is any of the coefficients $\chi_{\pm NL}(r_\perp)$, $\beta_\pm(r_\perp)$, $p_\pm(r_\perp)$, $r_\pm(r_\perp)$, $i=1,2,3,4$, and Δ_i is one of the following detunings:

$$
\begin{aligned}
&\Delta_1=-2\gamma-\chi_{+L}-\chi^*_{-L}, \quad \Delta_2=\chi_{+L}-\chi^*_{-L}, \\
&\Delta_3=-2\gamma-2\chi_{+L}, \quad \Delta_4=-2\gamma-2\chi^*_{-L}.
\end{aligned}
\tag{21}
$$

As a result, we obtain the set of eigenvalues

$$
\begin{aligned}
&\Gamma_1=\gamma+\chi_{+L}-\left[\int_{-\infty}^{\infty}\chi_{+NL}(r_\perp)dr_\perp\right]^2, \quad \Gamma_2=-\Gamma_1, \\
&\Gamma_3=\gamma+\chi^*_{-L}-\left[\int_{-\infty}^{\infty}\chi^*_{-NL}(r_\perp)dr_\perp\right]^2, \quad \Gamma_4=-\Gamma_3.
\end{aligned}
\tag{22}
$$

This discrete set of eigenvalues governs the spectral and spatial properties of FPS in the field of composed filaments. We will select those of them having a physical meaning and analyze them in the following section.

IV. MULTICONICAL EMISSION

First of all we should simplify the expression (12) for the susceptibility using the condition of the absence of linear absorption for all interacting waves: $\delta,|\delta\pm\epsilon|\gg 1$. In order to obtain an expression containing the Rabi resonance explicitly

we suppose also $|\epsilon| \gg 1$. Thus we temporarily exclude the Rayleigh-gain band at small $\epsilon < 0$ whose contribution will be estimated below.

Introducing the Rabi intensity $I_R = \eta(\epsilon^2 - \delta^2)/(4\delta^2)$ and the width of the Rabi resonance $\kappa = 1/2\epsilon(\eta + 2I_R[(\eta+1)/\eta])$ we can rewrite the expression for $\chi_+[\chi_-(\epsilon) = \chi_+(-\epsilon)]$ as a function of the intensity I:

$$\chi_+ = \frac{\rho_0}{\delta(1+4I_R)(1+\sqrt{1+4I_R/\eta})} \times \left[\frac{4I_R + (1+\sqrt{1+4I_R/\eta})/2}{\sqrt{1+4I}} + \sqrt{I_R}\frac{(1-\sqrt{1+4I_R/\eta})}{2\sqrt{I_R - I + i\kappa}} \right]. \tag{23}$$

It follows from the analysis of (23) that an emission with frequencies $\omega_+ > 2\omega_0 - \omega_{21}$, or $\epsilon > \delta$ will be amplified (Im $\chi_+ > 0$) for all values of I. At the same time the nonlinear addition to the refractive index proportional to $-[\mathrm{Re}\chi_+ - \rho_0/(\delta+\epsilon)]$ is always positive in the same conditions. That means the imaginary part of Γ_1 is positive for $\epsilon > \delta$.

Further, it is easy to show that the eigenvalue Γ_1 describes propagation of the beam F_+ at all coupling coefficients equal to zero. It has to be amplified because of the positive detuning from the pump frequency. As we can see from (13) the eigenvalue Γ_1 corresponds to the amplification as well and could be selected as the "right" eigenvalue for $\epsilon > \delta$.

The same procedure can be carried out with the other three eigenvalues. Finally, we choose eigenvalues Γ_1 and Γ_2, which have a physical meaning at $\epsilon > \delta$, and Γ_3 and Γ_4, which have to be selected at $\epsilon < -\delta$. Because of the symmetry we will consider only the case $\epsilon > \delta$.

The spatial distribution of the scattered emission can be obtained from Eqs. (14) at $\Gamma = \Gamma_{1,2}$. It is easy to show that the angle Θ between the axis $\pm z$ and the direction of propagation of the emission with frequencies on blue side of the resonant transition $\omega > 2\omega_0 - \omega_{21}$ takes two values:

$$\Theta = \Theta_1^{blue} \simeq 0, \quad \Theta = \Theta_2^{blue} \simeq \left(\frac{2}{k}\right)^{1/2} \sqrt{-2\gamma - 2\chi_{+L}}. \tag{24}$$

The angles of the emission with the frequency on the red wing $\omega < \omega_{21}$ are

$$\Theta = \Theta_1^{red} \simeq \left(\frac{2}{k}\right)^{1/2} \sqrt{-2\gamma - \chi_{+L} - \chi_{-L}},$$

$$\Theta = \Theta_2^{red} \simeq \left(\frac{2}{k}\right)^{1/2} \sqrt{\chi_{+L} - \chi_{-L}}. \tag{25}$$

Using the expressions for the linear susceptibilities we can write the angles of the cones explicitly:

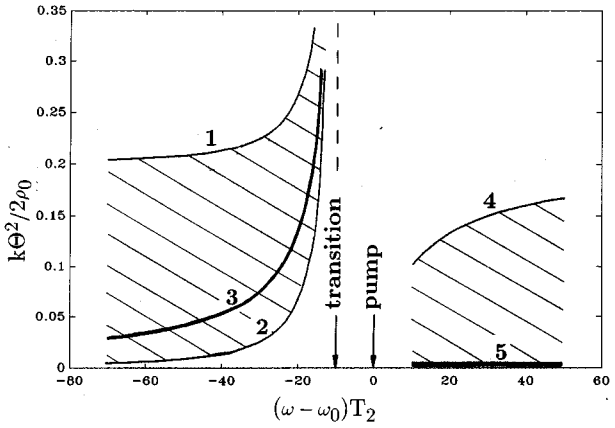

FIG. 2. Spectral dependences of the emission angles Θ of the scattered radiation. The pump is detuned on the blue side $\delta = 10$ of the resonant transition. The curves 1 and 2 are upper (weak saturation) and lower (strong saturation) boundaries for the angle Θ_2^{red} expected in an experiment; the curve 3 corresponds to conical emission under angle Θ_1^{red}. The curve 4 shows an upper limit for angles Θ_2^{blue} and the curve 5 illustrates an emission trapped by the filament.

$$\frac{k(\Theta_1^{red})^2}{2\rho_0} = -2\frac{\gamma}{\rho_0} + \frac{2\delta}{\epsilon^2 - \delta^2}, \frac{k(\Theta_2^{red})^2}{2\rho_0} = \frac{2\epsilon}{\epsilon^2 - \delta^2},$$

$$\frac{k(\Theta_2^{blue})^2}{2\rho_0} = -2\frac{\gamma}{\rho_0} - \frac{2}{\epsilon + \delta}. \tag{26}$$

The spectral dependences of the cone angles are shown in Fig. 2. The value γ depends on the energy of the CF [15], and it can take any value between $-\rho_0/\delta$ (weak saturation) and 0 (strong saturation). In an experiment, if the input strong laser beams are broken up into a set of CF's with different energies, the conical emission under angles Θ_2^{red} and Θ_2^{blue} produces in the far field a blurred ring and circle, respectively. That is shown in Fig. 2 as the dashed bands. In the case of a single CF, because of uncertainty in the value of

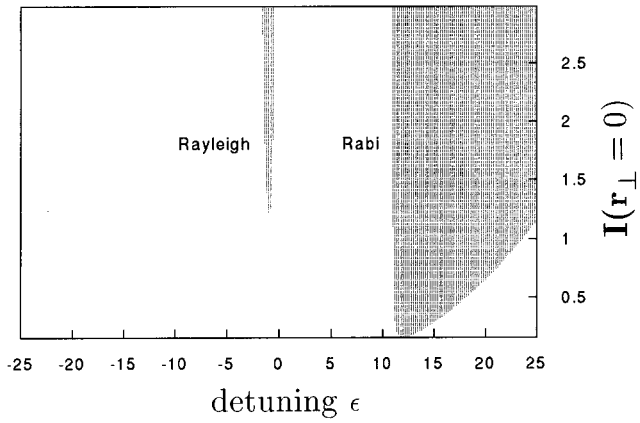

FIG. 3. Diagram of the frequency-shifted instability of the composite filament with the Gaussian shape $I(r_\perp) = I(r_\perp = 0)\exp(-r_\perp^2)$ at $\delta = 10, \eta = 1$. The dashed regions correspond to a gain Im $\Gamma_1(\epsilon; I(r_\perp = 0)) < 0$.

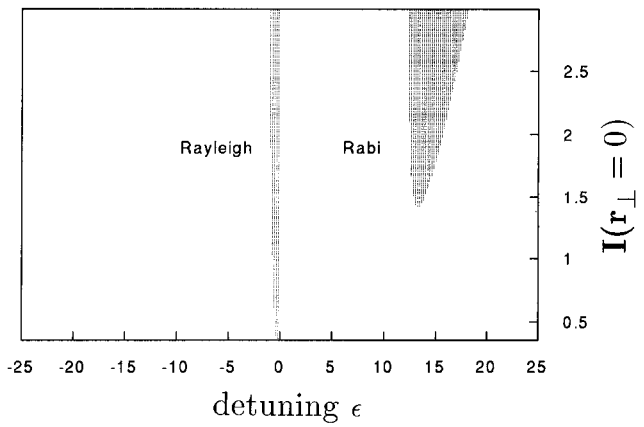

FIG. 4. The same as in Fig. 3 at $\eta=5$.

γ, the bands can be considered as the domains of credibility for the cone angles Θ_2^{red} and Θ_2^{blue}. The emission going along the z axis $\Theta_1^{blue}=0$ and to a cone under the angle Θ_1^{red} results in a well resolved central spot on the blue side and a ring on the red side of the resonant transition.

It should be noted also that the intensity of the multiconical emission does depend on the frequency ω of the scattered radiation. The analysis of this is restricted by the uncertainty in the CF's form and energy. We can just recall the experimental results on conical emission at copropagation (see an overview in [11]), where the most intense conical emission is usually detected for $\omega=2\omega_{21}-\omega_0$.

Figure 2 is close to an experimental situation in the sense that the scattered frequencies and corresponding angles can be measured directly from an experiment. It displays the characteristics of the multiconical emission integrated on the filament's parameters, and shows, for example, the range of frequencies where the multiconical emission can be excited. More precise information is given by the instability diagram derived from the equation $\mathrm{Im}\Gamma_j(\mathbf{P})=0$ mentioned above. Such diagrams with pump intensity $I(r_\perp=0)$ on the filament's axis and detuning ϵ taken as the components of the vector $\mathbf{P}$ are shown on Figs. 3 and 4. For simplicity we have chosen a Gaussian profile of the CF: $I(r_\perp)=I(r_\perp=0)\exp(-r_\perp^2)$.

The presence of two gain bands in the spectrum is clearly seen from Figs 3 and 4: a Rayleigh one positioned at small $\epsilon<0$, and a Rabi one at $\epsilon>\delta$. Such a situation is quite similar to the problem of competition between Rayleigh and Rabi instabilities of counterpropagating plane waves raised in [3,18]. The preferable excitation of the Rayleigh band observed in [3] was explained in [18] as a consequence of the suppression by a high buffer gas concentration of the Rabi gain. The same effect is produced in our case of spatially inhomogeneous pumping. As follows from a comparison of Figs. 3 and 4, an increase of the buffer gas pressure (Fig. 3 $T_1=T_2$ and Fig. 4 $T_1=5T_2$) results in a drastic change of the relation between threshold values for Rabi and Rayleigh instabilities: the latter is excited first with increase of the pump intensity in a high buffer gas pressure domain.

We should note that the linear absorption $\mathrm{Im}\chi_{\pm L}$ was considered as an independent parameter due to the fact that the filament's transverse size affects only the integral part of the eigenvalues (22). In order to make the stability diagrams more illustrative, its value has been chosen quite small, which allows the nonlinear gain to predominate over the linear absorption even at small pump intensities $I(r_\perp=0)$. That explains the closeness of the convective instability regions in Fig. 3 to the axis $I(r_\perp=0)=0$. Contact can occur only in the physically unacceptable case of neglect of the linear absorption.

Nevertheless, as can be shown, the Rayleigh instability does not produce sufficient cone angles as the Rabi one does. That means that the FPS enhanced by only the Rabi gain is responsible for the multicone structure of the scattered radiation in the field of counter-propagating composite filaments.

V. CONCLUSIONS

We have shown that the formation of composite filaments consisting of two counter-propagating components can be considered as an intermediate state in the development of instability of counterpropagating light beams in resonant media. We analyzed only one of possible ways of formation of the CF's, namely, via attraction and unification of counterpropagating filaments already created as a result of self-focusing of opposite light beams. That happens if the interaction between counterpropagating beams is weaker (or delayed in time) than the self-action processes, and the total dynamics in some sense can be decoupled in the two subsystems. Intuitively, that is possible at quite large interaction lengths L. The counter-propagation in short resonant media exhibits an instability of the input plane waves usually leading to formation of hexagon patterns in a transverse section [5]. An increase of the medium length, which plays the role of a critical parameter, leads to an enhancement of spatial inhomogeneousity and to instability processes which can be analyzed already from the point of view of collective dynamics of filaments (spots in a transverse section), initially organized into a hexagonal lattice. So the system far away from the static instability threshold should form composite filaments which are stable with respect to frequency-degenerate spatial perturbations.

Hence, the following stage is the four-photon frequency-nondegenerate instability of the CF exhibited as multiconical emission. As has been shown, it consists of a central spot and cone on the blue side of the resonant transition and two cones on the red side in the farfield. The asymmetry in angles of emission of the radiation components coupled via FPS and distributed feedback reflection displays the main observable consequence of the spatially unhomogeneous pumping. That happens thanks to the fact that only emission with frequency on the blue side can be trapped by the filament, acting as a waveguide. Another part of the scattered radiation which appears due to the four-photon interaction can propagate in fixed directions ruled by wave-vector matching conditions (Cherenkov's at co-propagation).

The results presented are obtained in the framework of the single-mode approximation corresponding to a weak four-photon gain of the scattered emission. The growth of intensity and transverse size of the pump beams will lead to the appearance of new eigenvalues and consistently to an in-

creasing number of cones. As shown in a WKB approximation for the case of copropagation [11], the cones angle values stop obeying the phase matching conditions, and can sufficiently exceed those predicted by one or another synchronism rule.

ACKNOWLEDGMENTS

The authors would like to acknowledge Professor W. J. Firth for useful discussions. B. A. Samson thanks the Royal Society of London for financial support.

[1] I. Bar-Joseph and Y. Silberberg, Phys. Rev. A **36**, 1731 (1987).
[2] G. Giusfredy, J.F. Valley, R. Pon, G. Khitrova, and H.M. Gibbs, J. Opt. Soc. Am. B **5**, 1181 (1988).
[3] G. Khitrova, J.F. Valley, and H.M. Gibbs, Phys. Rev. Lett. **60**, 1126 (1988).
[4] C.T. Law and A.E. Kaplan, Opt. Lett. **14**, 734 (1989).
[5] G. Grynberg, R. Le Bihan, P. Verkerk, P. Simoneau, J.R.R. Leite, D. Bloch, S. Le Boiteux, and M. Ducloy, Opt. Commun. **67**, 363 (1988).
[6] A. Petrossian, M. Pinard, A. Maitre, J.-Y. Courtois, and G. Grynberg, Europhys. Lett. **18**, 689 (1992).
[7] J.V. Moloney, H. Adachihara, R. Indik, C. Lizarraga, R. Northcutt, D.W. McLaughlin, and A.C. Newell, J. Opt. Soc. Am. B **7**, 1039 (1990).
[8] W.J. Firth, and C. Pare, Opt. Lett. **13**, 1096 (1988).
[9] G. Grynberg, A. Maitre, and A. Petrossian, Phys. Rev. Lett. **72**, 2379 (1994).
[10] D.J. Harter and R.W. Boyd, Phys. Rev. A **29**, 739 (1984).
[11] A.A. Afanas'ev, B.A. Samson, and R. Yakite, Laser Phys. **1**, 399 (1991).
[12] J.F. Valley, G. Khitrova, H.M. Gibbs, J.W. Grantham, and Xu Jiajin, Phys. Rev. Lett. **64**, 2362 (1990).
[13] H.E. Ponath, U. Trutschel, U. Langbein, and F. Lederer, J. Opt. Soc. Am. B **5**, 539 (1988).
[14] J.E. Bjorkholm, P.W. Smith, W.J. Tomlinsen, and A.E. Kaplan, Opt. Lett. **6**, 345 (1981); A.E. Kaplan, *ibid.* **6**, 360 (1981).
[15] A.A. Afanas'ev and B.A. Samson, Phys. Lett. A **166**, 49 (1992).
[16] P.A. Apanasevich, A.A. Afanas'ev, and B.A. Samson, Izv. Akad. Nauk SSSR Ser. Fiz., **51**, 270 (1987) [Bull. Acad. Sci. USSR Phys. Ser. **51**, 58 (1987)].
[17] M. Le Berre, E. Ressayre, and A. Tallet, Phys. Rev. A **43**, 6345 (1991).
[18] M. Le Berre, E. Ressayre, and A. Tallet, Phys. Rev. A **46**, 4123 (1992).
[19] M. Le Berre, E. Ressayre, and A. Tallet, Opt. Commun. **87**, 358 (1992).
[20] M. Le Berre, E. Ressayre, and A. Tallet, Phys. Rev. A **44**, 5958 (1991).